Bioorganic Chemistry 87 (2019) 523–533

Contents lists available at ScienceDirect

Bioorganic Chemistry

journal homepage: www.elsevier.com/locate/bioorg

Natural product-based design, synthesis and biological evaluation of 2′,3,4,4′-tetrahydrochalcone analogues as antivitiligo agents

Hui Zhong[a], Jia Zhou[a,*], Xiao-Hong An[a], Ying-Rong Hua[a], Yi-Fan Lai[a], Rui Zhang[a], Owais Ahmad[a], Ye Zhang[b,c,*], Jing Shang[a,*]

[a] State Key Laboratory of Natural Medicines, Jiangsu Key Laboratory of TCM Evaluation and Translational Research, School of Traditional Chinese Pharmacy, China Pharmaceutical University, Nanjing 211198, China
[b] School of Pharmacy, Guilin Medical University, Guilin 541004, China
[c] State Key Laboratory for Chemistry and Molecular Engineering of Medicinal Resources, School of Chemistry and Pharmacy, Guangxi Normal University, Guilin 541004, China

ARTICLE INFO

Keywords:
2′,3,4,4′-Tetrahydrochalcone
Vitiligo
Oxidative stress
MAPK
C-kit

ABSTRACT

A bioactive component, 2′,3,4,4′-tetrahydrochalcone (**RY3-a**) was first isolated from *Vernohia anthelmintica (L.) willd* seeds, and a set of its analogs, **RY3-a-1–RY3-a-15** and **RY3-c** were designed and synthesized. Biological activity assays showed that **RY3-c** exhibited better melanogenesis and antioxidant activity and lower toxicity in comparison with **RY3-a** and butin. Further study tests showed that **RY3-c** exhibited better melanogenesis activity compared with the positive control 8-methoxypsoralan (8-MOP) in a vitiligo mouse model, suggesting that **RY3-c** is a good candidate antivitiligo agent. Mechanistic studies showed that **RY3-c** could repair cell damage induced by excessive oxidative stress and may exert melanin synthesis activity in the mouse melanoma B16F10 cell line by activating the mitogen-activated protein kinase (MAPK) pathway and the upregulation of c-kit.

1. Introduction

As a disease affecting 1–4% of the world's population, vitiligo is a depigmenting disorder of the skin and hair follicles characterized by the destruction of the melanocytes, mainly exhibiting clinical manifestation as expanding hypopigmented lesions of the skin [1]. The pathobiology of vitiligo has been debated for the last six decades, and remains obscure [1,2]. The absence of melanocytes in the skin lesion due to their destruction is suggested to be the key event in the pathogenesis of vitiligo [3]. Previous work has indicated that oxidative stress could be considered as one of the important pathogenic events in melanocyte loss [4,5]. In addition, systemic oxidative stress has been widely reported in vitiligo patients [6–8]. Moreover, a previous study has also suggested oxidative stress as the initial triggering factor in precipitating vitiligo [6]. Therefore, oxidative stress is now seriously considered to be the main pathogenic event in vitiligo [6,9]. Oxidative stress may induce and mediate multiple genes encoding proteins through several signaling pathways, including tyrosinase (TYR), microphthalmia-associated transcription factor (MITF), and MAPK, and ultimately leads to melanin loss and vitiligo [10]. It is thus widely considered that antioxidant intervention should improve the level of oxidative stress, which may consequently play an important role in the prevention and treatment of vitiligo [11]. The potent antivitiligo effect of *Gingko biloba* [12] inspired us to screen for antivitiligo agents from traditional Chinese medicinal herbs, which are considered to be an important natural biological drug library and include antioxidant agents. In the search for new antivitiligo agents with high efficacy and low/no toxicity, considerable attention to antivitiligo herbs or formulas derived from traditional Chinese medicine herbs is now considered to be a reasonable research option.

Vernohia anthelmintica (L.) willd, which is an annual Chinese medicinal herb plant of asteraceae, has been used as a traditional Uyghur medicine (TUM) for vitiligo treatment since 1763 [13]. As a common drug for the treatment of vitiligo, *Vernohia anthelmintica (L.) willd* seeds exhibit a significant effect in the treatment of melanin deficiency and vitiligo [14,15]. To identify the active constituents responsible for the treatment of melanin deficiency and vitiligo in this herb, the extraction, separation and synthesis of medicinal components from *Vernohia anthelmintica (L.) willd* seeds has been performed. Previous work has indicated that the methanol and chloroform fractions of *Vernohia anthelmintica (L.) willd* seeds exhibit significant antioxidant activities, and flavonoids may be the active constituents responsible for the treatment of melanin deficiency and vitiligo [16]. Recently, a bioactive

* Corresponding authors at: State Key Laboratory of Natural Medicines, Jiangsu Key Laboratory of TCM Evaluation and Translational Research, School of Traditional Chinese Pharmacy, China Pharmaceutical University, Nanjing 211198, China. School of Pharmacy, Guilin Medical University, Guilin 541004, China.
E-mail addresses: cpuzj_2016@163.com (J. Zhou), zhangye81@126.com (Y. Zhang), shangjing21cn@163.com (J. Shang).

https://doi.org/10.1016/j.bioorg.2019.03.054
Received 2 November 2018; Received in revised form 19 February 2019; Accepted 18 March 2019
Available online 23 March 2019
0045-2068/

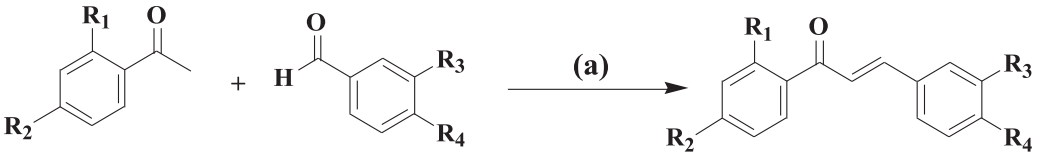

RY3-a:R_1=R_2=R_3=R_4=OH
RY3-a-1:R_1=R_2=R_4=OH, R_3=H
RY3-a-2:R_1=R_2=R_3=OH, R_4=H
RY3-a-3:R_1=R_2=OH, R_3=R_4=H
RY3-a-4:R_1=H, R_2=R_3=R_4=OH
RY3-a-5:R_2=H, R_1=R_2=R_3=OH
RY3-a-6:R_1=R_2=H, R_3=R_4=OH
RY3-a-7:R_1=R_3=OH, R_2=R_4=H
RY3-a-8:R_1=R_4=OH, R_2=R_3=H
RY3-a-9:R_1=R_2= R_3=H, R_4=OH
RY3-a-10:R_2=R_3=OH, R_1=R_4=H
RY3-a-11:R_1=R_3=OH, R_2=R_4=H
RY3-a-12:R_1=R_2=R_4=H, R_3=OH
RY3-a-13:R_1=R_3=R_4=H, R_4=OH
RY3-a-14:R_2=OH, R_2=R_3=R_4=H
RY3-a-15:R_1=R_2= R_3=R_4=H

Scheme 1. Synthetic route of compound **RY3-a**. Reagents and conditions: (a) 60% KOH, EtOH.

component butin has been isolated from *Vernohia anthelmintica (L.) willd* seeds and was reported to exhibit potent antivitiligo activity in a mouse model [17]. However, to the best of our knowledge, not all of the bioactive components have been isolated, and the antivitiligo activities and the action mechanisms have not been completely investigated. Herein, the isolation and separation of the active constituents form *Vernohia anthelmintica (L.) willd* seeds was thus performed. In the present work, the flavonoid compound 2′,3,4,4′-tetrahydrochalcone (**RY3-a**) was first isolated from *Vernohia anthelmintica (L.) willd* seeds. A biological evaluation assay showed that 2′,3,4,4′-tetrahydrochalcone exhibited increased antivitiligo activity and no significant toxicity in comparison with butin. However, due to low yield of 2′,3,4,4′-tetrahydrochalcone from the plant material, we accomplished its total synthesis, which enabled us to synthesize sufficient compounds for further biological studies. In addition, the significant antivitiligo activity, structural simplicity and low toxicity of 2′,3,4,4′-tetrahydrochalcone also greatly encouraged us to design and synthesize additional 2′,3,4,4′-tetrahydrochalcone analogs as antivitiligo agents. Thus, a set of 2′,3,4,4′-tetrahydrochalcone analogs (**RY3-a-1–RY3-a-15,** Scheme 1) were designed and synthesized as antivitiligo agents in the present work based on the skeleton of 2′,3,4,4′-tetrahydrochalcone. Unfortunately, preliminary zebrafish model assay results showed that all of the synthetic 2′,3,4,4′-tetrahydrochalcone analogs, **RY3-a-1–RY3-a-15,** exhibited lower melanin synthesis activity than **RY3-a**, and some of the analogs (those with the presence of OH near the carbonyl group) exhibited increased toxicity. Through the study of the structure-activity relationship of **RY3-a,** its analogs and butin, the tetrahydro-4-pyrone ring of butin and the conjugated ketene skeleton of **RY3-a** analogs inspired us to construct a dihydro-4-pyranone ring (Fig. 1) in the **RY3-a** moiety and to remove the OH near the carbonyl group. Previous work has indicated that cyclic flavone derivatives usually exhibited good antioxidant activity, and it was thus expected that the combination of tetrahydro-4-pyrone and the conjugated ketene skeleton may lead to good antioxidant activity and consequently potential antivitiligo activity. Thus, a flavone compound (**RY-3-c**) was finally designed and synthesized as an antivitiligo agent based on the 2′,3,4,4′-tetrahydrochalcone framework (Scheme 2). Antivitiligo activity screening results showed that in comparison with **RY-3-a** and **RY-3-b**, **RY-3-c** exhibited increased antioxidant and antivitiligo activities and lower toxicity. Further tests showed that **RY3-c** exhibited better melanogenesis activity compared with the commercial antivitiligo drug 8-methoxypsoralan (8-MOP) in a vitiligo mouse model, suggesting that **RY3-c** should be a good candidate for an antivitiligo agent, which is consistent with our expectation. In addition, our preliminary mechanistic study showed that **RY3-c** could repair cell damage induced by excessive oxidative stress. Moreover, further investigation into the mechanism of action revealed that **RY-3-c** may exert antivitiligo activity via MAPK signaling, providing good proof-of-concept for our network pharmacological prediction studies in the present work.

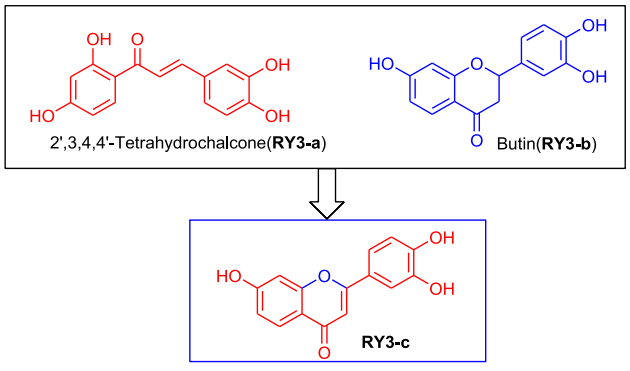

Fig. 1. Design of compound **RY-3c**.

2. Results and discussion

2.1. Chemistry

2′,3,4,4′-Tetrahydrochalcone, isolated as a yellow amorphous powder, showed a molecular ion peak at *m/z* 271 in its HREI-MS, indicating a molecular formula of $C_{15}H_{12}O_5$ (calcd for [M-H], 271). Its NMR spectra exhibited the presence of four hydroxyl groups [δ_H = 13.62, 10.68, 9.78, 9.12 and δ_C = 113.35, 148.53, 164.94, 166.10], six aromatic protons [δ_H = 7.72, 7.33, 6.87, 6.45, 6.34 and δ_C = 114.45, 113.35, 115.24, 116.96, 127.07, 131.88], one carbonyl group [δ_C = 192.13] and one olefin group [δ_H = 8.19, 7.26 and δ_C = 107.75, 144.69]. These data, together with comparison with the NMR data of the known 2′,3,4,4′-tetrahydrochalcone, established the structure of compound **RY-3a**, named 2′,3,4,4′-tetrahydrochalcone [18]. The low yields of 2′,3,4,4′-tetrahydrochalcone in *Vernohia anthelmintica (L.)* willd seed prompted us to design, synthesize and explore a simple and efficient synthetic route for 2′,3,4,4′-tetrahydrochalcone as well as a synthetic method for its analogues. The synthetic routes are shown in Scheme 1 (compounds **RY3-a**, **RY3-a-1–RY3-a-15**).

As shown in Scheme 1, 2′,3,4,4′-tetrahydrochalcone (**RY3-a**) and its derivatives (**RY3-a-1–RY3-a-15**) were synthesized through a Claisen-Schmidt reaction [19–21] by the combination of corresponding 2,4-dihydroxyacetophenone derivatives and protocatechualdehyde derivatives, respectively.

By the analysis of the structure-activity relationship of **RY3-a** and its derivatives and butin, a 2′,3,4,4′-tetrahydrochalcone analog **RY3-c** was then designed and synthesized as described in Scheme 2. As shown in Scheme 2, **RY3-c-1**, which was synthesized by the treatment of 3,4-dihydroxyl-ethyl benzoate and benzyl bromide in the presence of potassium, was treated with 2,4-dihydroxyl-benzophenone to afford **RY3-c-2**. The treatment of **RY3-c-2** with Dowex-H^+ resin in the presence of 2-propanol provided compound **RY3-c-3**, which was finally hydrolyzed to afford **RY3-c** in the presence of 40% potassium hydrate.

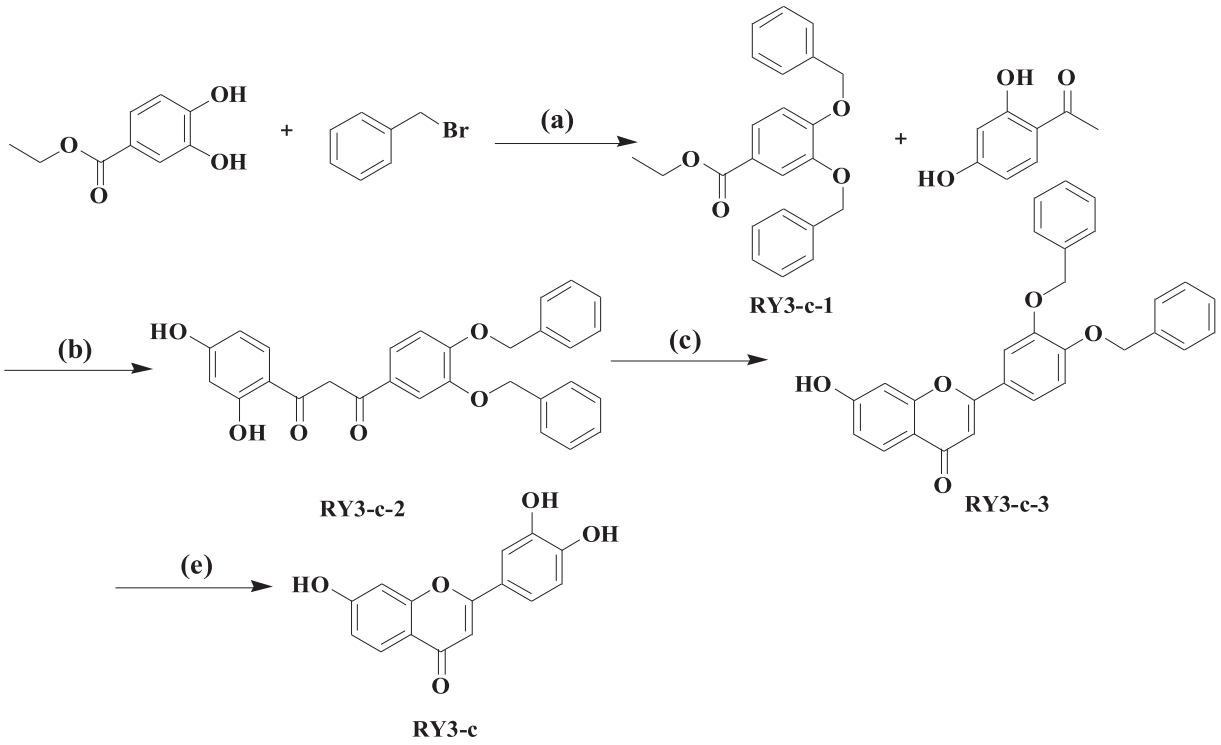

Scheme 2. Synthetic route of compound **RY3-c**. Reagents and conditions: (a) PhBr, K_2CO_3, CH_2Cl_2; (b) LiHMDS, tetrahydrofuran (THF), −60 °C; (c) Dowex-H^+, 2-propanol, reflux; (d) Pd-C, H_2, MeOH.

The structures of all of the target compounds (**RY3-a**, **RY3-a-1–RY3-a-15** and **RY3-c**) were confirmed by ^{1}HNMR, ^{13}CNMR and high resolution mass spectrometry (HRMS) (Part 4 of the Supplementary Data).

2.2. Evaluation of the antivitiligo and antioxidant activities

2.2.1. Melanogenesis and tyrosinase enzymatic activities in zebrafish

Due to the melanin pigments in their skin, zebrafish have been considered an efficient whole-animal model for screening melanogenic inhibitors or stimulators [22]. Changes in the melanin content and tyrosinase enzymatic activity are the most visual indices to evaluate the movement of molecules. In general, cutaneous melanin can be first observed at 24 hpf in the zebrafish retina, and alterations in the tyrosinase enzymatic activity can be detected at 21 hpf [23]. To better identify the changes in melanin content and tyrosinase enzymatic activity, the well-known melanogenic inhibitor 1-phenyl-2-thiourea (PTU) was used to build the pigment model. As shown in Fig. 2A, compared to the control group and the PTU-2 group, the melanin content of zebrafish treated with PTU decreased significantly from 6 hpf to 60 hpf. In the PTU-2 group, zebrafish were treated with PTU from 6 hpf to 35 hpf and then water. The melanin content of zebrafish in this group was more than that of the PTU-1 group but less than that of the control group. Fig. 2A also shows that the depigmentation model of zebrafish, which involved treatment with PTU, was safe and effective. As shown in Fig. 2A, compounds **RY3-a**, **RY3-a-1**, **RY3-a-4**, **RY3-a-7** and **RY3-a-10** significantly increased melanin content in zebrafish, while compounds **RY3-a-3**, **RY3-a-5**, **RY3-a-6**, **RY3-a-9**, **RY3-a-12**, **RY3-a-14** and **RY3-a-15** could not increase melanin synthesis in zebrafish, indicating that **RY3-a**, **RY3-a-1**, **RY3-a-4**, **RY3-a-7** and **RY3-a-10** may be good melanogenic stimulators. Evidently, among all of these compounds, **RY3-a** exhibited the best stimulating activity for melanosynthesis. It was important to note that treatment with **RY3-a-3, RY3-a-5, RY3-a-8** and **RY3-a-14** led to the morphological deformity of zebrafish, indicating that these compounds exhibited obvious toxicity. This result also implied that the presence of a hydroxyl group in the R_1 position (near the carbonyl group) may lead to serious toxicity and thus should be removed.

Based on the above observation, it should be concluded that this structural modification of 2′,3,4,4′-tetrahydrochalcone did not improve the activities of melanotropins, and the presence of a hydroxyl group in the R_1 position may even increase its toxicity. Thus, as described in the Introduction section, the 2′,3,4,4′-tetrahydrochalcone analog **RY3-c** was designed and synthesized to improve the activities of melanotropin and the toxicity by the combination of **RY3-a** and butin. The melanotropin and tyrosinase enzymatic activities of **RY3-c** were then assayed using **RY3-a** and **RY3-b** (butin) as the positive controls.

As shown in Fig. 3A–C, in comparison with the PTU-2 group, the changes in the melanin content of the entire zebrafish body, and particularly those of the retina and dorsolateral skin, showed that **RY3-a**, **RY3-b** and **RY3-c** significantly increased melanin synthesis in zebrafish in a dose-dependent manner. It was worth noting that **RY3-c** exhibited the highest melanotropin activity among these three compounds. The tyrosinase activities of zebrafish treated with **RY3-a**, **RY3-b** and **RY3-c** were also measured. It is important to note that, as shown in Fig. 3D, both **RY3-a** and **RY3-c** significantly increased the tyrosinase activity at concentrations of 20 μM and 40 μM in comparison with the PTU-2 group, while **RY3-c** exhibited higher tyrosinase activity. In the **RY3-b** treatment group, there was no significant difference after **RY3-b**-treatment (1, 10, 20, and 40 μM) compared with the PTU-2 group. Thus, it was obvious that **RY3-c** exhibited the greatest melanogenic and tyrosinase enzymatic stimulating activities of these three compounds.

2.2.2. Melanogenesis activity quantified by TYR and MITF

As the rate-limiting enzyme, TYR can convert tyrosine to L-3,4-dihydroxyphenylalanine, dopaquinone, dopachrome and subsequently melanin during the production of melanins [24]. In addition, MITF is the major transcription factor for the upregulation of the transcription of melanin genes and the expression of the melanogenic enzyme [25]. Thus, the expression levels of TYR and MITF should be quantified as the unique detection indices of melanogenesis [26,27]. To evaluate the melanogenesis activity, B16F10 cells were treated with **RY3-a**, **RY3-b**

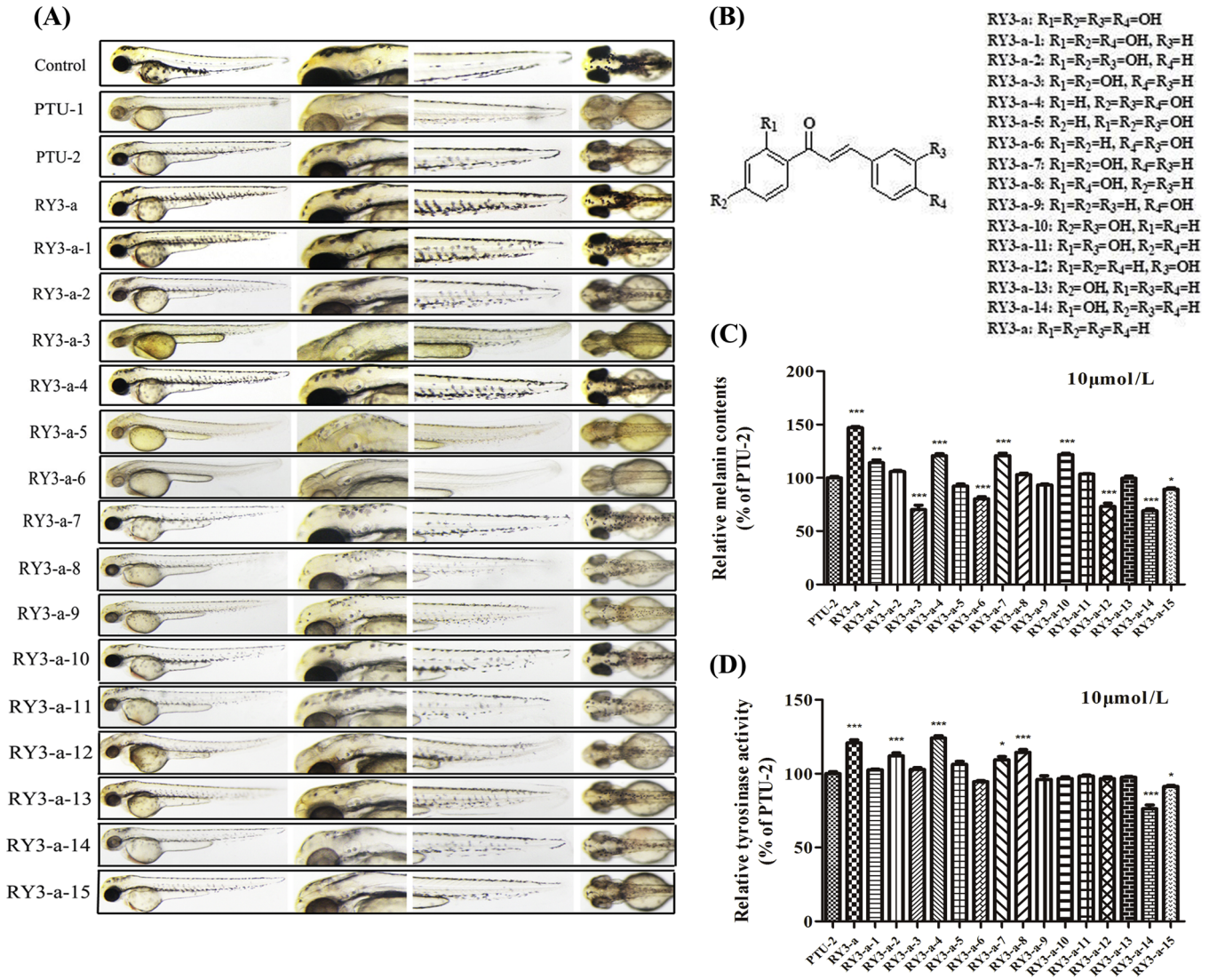

Fig. 2. Melanogenesis and tyrosinase enzymatic activities of **RY3-a** derivatives in the zebrafish model.

and **RY3-c** for 48 h, and Fontana-Masson staining was performed. As shown in Fig. 4, all of these compounds increased melanogenesis in B16F10 cells, while **RY3-a** and **RY3-c** exhibited higher melanogenesis activity than **RY3-b**. In addition, Fig. 4 also shows that both **RY3-a** and **RY3-c** promoted melanin transfer from the area near the nucleus to the surrounding membrane area and to the dendrite tips, in particular, indicating that **RY3-a** and **RY3-c** not only promoted melanin synthesis but also stimulated melanin translocation.

To further evaluate the melanogenesis activity, the in vitro expression levels of TYR and MITF were then investigated by western blot assays. As shown in Fig. 5, it was evident that the expression levels of MITF and TYR remarkably increased in B1F10 cells by treatment with **RY3-c** at concentrations of 0.1 μM, 1 μM and 10 μM. However, in the **RY3-a** and **RY3-b** treatment groups, **RY3-a** and **RY3-b** only increased the expression levels of MITF at a concentration of 10 μM. The data strongly suggested that **RY3-c** exhibited the best efficacy towards melanogenesis, which is consistent with the above melanogenesis and tyrosinase enzymatic activity assay results.

2.2.3. *Toxicity tests in the zebrafish model*

Previous studies have shown that in comparison to the human reference genome, approximately 70% of human genes have at least one obvious zebrafish orthologue [28]. Thus, zebrafish (*Danio rerio*) has been considered a genetically tractable organism with similarities to humans. Zebrafish have been used for chemical toxicity testing since 1965 [29]. It is known that 24 hpf is at the end segmentation stage from embryos to larvae, and the time points of 48 hpf, 72 hpf, 96 hpf, and 120 hpf are specified time points during the developmental progression of zebrafish. Therefore, the mortality of zebrafish should be recorded at these time points [30]. Body length and morphology deformity assessments are the major testing indices for toxicity tests; they should be observed and photographed at the time points specified above. Therefore, the toxicity of **RY3-a** was observed in zebrafish, and malformations were photographed. As shown in Fig. S1-1.A (Supplementary Data (Part 1)), pericardial edema was observed at the concentration of 100 μM at 96 hpf, while significant malformations were evident at the concentration of 150 μM from 48 hpf to 120 hpf. As shown in Fig. S1-1D, in the **RY3-b** treatment group, pericardial edema was observed at the concentration of 50 μM at 120 hpf, and significant malformations were obvious at the concentration of 100 μM from 48 hpf to 120 hpf. It was worth noting that, as shown in Fig. S1-1G, pericardial edema in the **RY3-c**-treated group was observed even at the concentration of 200 μM at 120 hpf. The body length and morphology deformity assessments above showed that **RY3-c** exhibited the lowest toxicity in zebrafish, while **RY3-b** exhibited the highest toxicity. As shown in Fig. S1-1B, Fig. S1-1E, Fig. S1-1H, Fig. S1-1C, Fig. S1-1F, and Fig. S1-1I, taking the

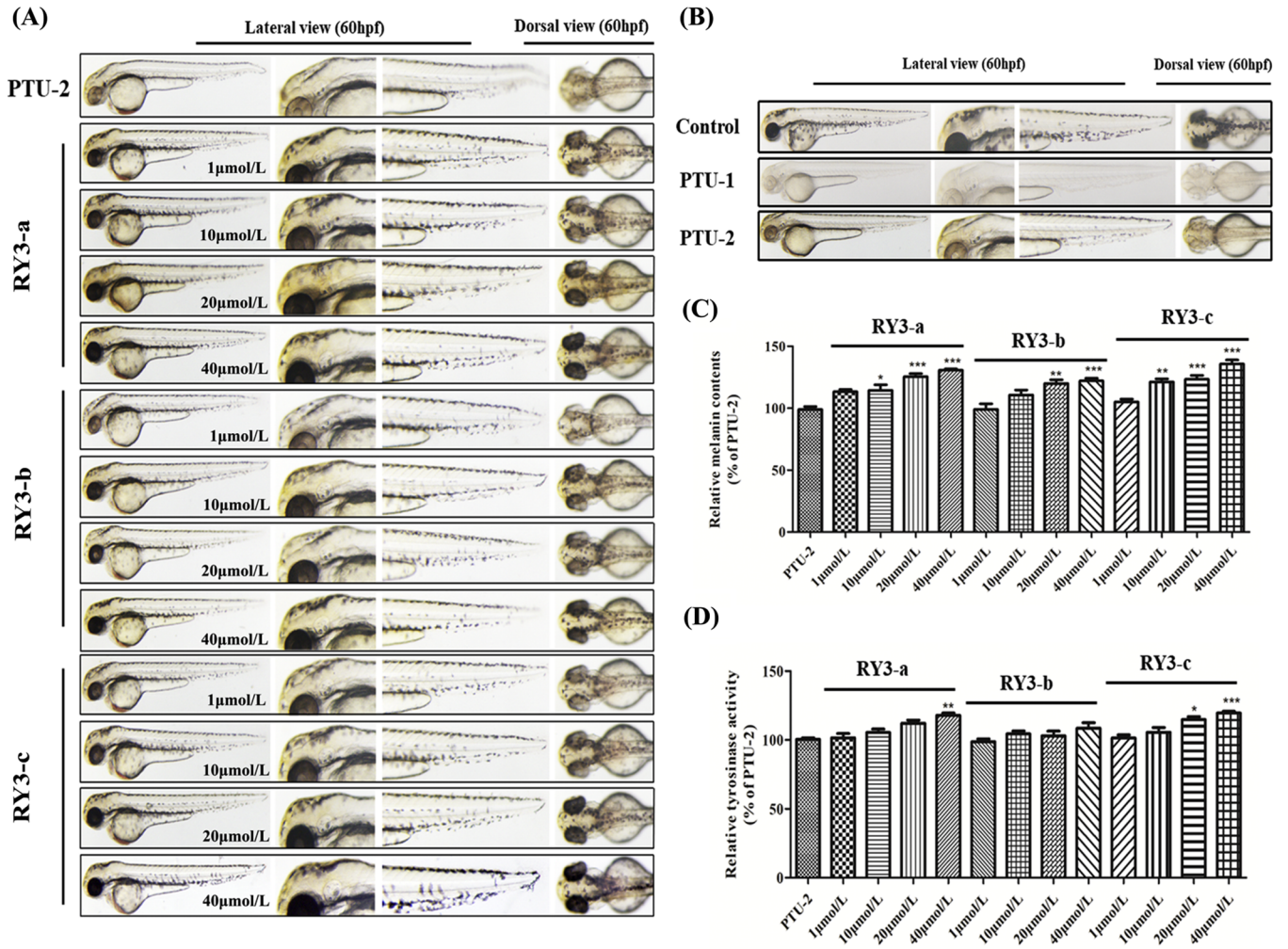

Fig. 3. Melanogenesis and tyrosinase enzymatic activities of **RY3-a**, **RY3-b** and **RY3-c** in the zebrafish model. (A) Zebrafish were treated with PTU (0.2 mM) from 6 hpf to 35 hpf, and then, PTU was changed to water for another 25 h (from 35 hpf to 60 hpf) in the PTU-2 group. In the PTU-1 group, zebrafish were treated with PTU (0.2 mM) from 6 hpf to 60 hpf, while water was used in the control group. (B) Zebrafish were treated with PTU (0.2 mM) from 6 hpf to 35 hpf, and then, PTU was changed to water containing different doses of **RY3-a**, **RY3-b** and **RY3-c** for another 25 h (from 35 hpf to 60 hpf). **RY3-a**, **RY3-b** and **RY3-c** increased melanin recovery. (C) A homogenate of each group of zebrafish was used to examine melanin content. (D) A homogenate of each group of zebrafish was used to examine the tyrosinase activity. Data were analyzed by one-way analysis of variance (ANOVA) followed by the post hoc Tukey test. $^{*}P < 0.05$, $^{**}P < 0.01$, compared with PTU-2.

survival and body length of the zebrafish as indices, there were no significant differences after **RY3-c** treatment (1, 10, 50, and 100 μM) in comparison with the control group at 24, 48, 72, 96 and 120 hpf. The survival rate and the body length of zebrafish were significantly changed at the concentration of 100 μM in the **RY3-a** treatment group, and changes in the **RY3-b** treatment group also appeared at the concentration of 100 μM. The results also confirmed that **RY3-c** exhibited the lowest toxicity in zebrafish.

In brief, the high melanogenic activity and the low toxicity of **RY3-c** rendered it a good candidate as an antivitiligo agent. Thus, **RY3-c** was selected for further investigation in a mouse model.

2.2.4. Effect of RY3-c on melanin synthesis in the vitiligo mouse model induced by hydroquinone

The mouse model of vitiligo induced by hydroquinone has been widely used for screening antivitiligo agents [31,17]. Forty-eight male C57BL/6 mice were randomly divided into four groups. Ointments including hydroquinone, the commercial antivitiligo drug 8-MOP and **RY3-c** were studied, and the formulations of the ointments are described in the Supplementary Data (Part 2). Hair was removed via shaving (1.5 × 1.5 cm) the dorsal skin of the mice. The control group was treated with placebo ointment, and the model group was treated with 2.5% hydroquinone, which was dispersed well in excipient once daily for 40 days after hair removal.

As shown in Fig. 6, compared with the control group, the whitening of the dorsal skin in mice was obviously increased by hydroquinone treatment. Treatments with 8-MOP (8.5 μg/day) and **RY3-c** (10 μg/day) were performed for 40 days, respectively. The hair color of mice in the 8-MOP treatment group and **RY3-c** treatment group turned significantly darker compared with the model group. As shown in Fig. S1-2 (Supplementary Data (Part 1)), the effects of **RY3-c** on the numbers of melanin-containing epidermal cells, melanin-containing follicles and the basal melanocytes in the shaved skin areas of the mice were observed by hematoxylin and eosin staining. The model group showed a significant decrease in melanin-containing follicles compared with the control group, and the number of melanin-containing hair follicles in the treatment areas were significantly increased for the 8-MOP and **RY3-c** treatment groups, indicating high melanogenic activity of **RY3-c**. Obviously, **RY3-c** even exhibited higher melanogenic activity than 8-MOP, indicating that **RY3-c** is a good modulator of melanogenesis. This result was highly consistent with those of the zebrafish model and the B16F10 cell assays.

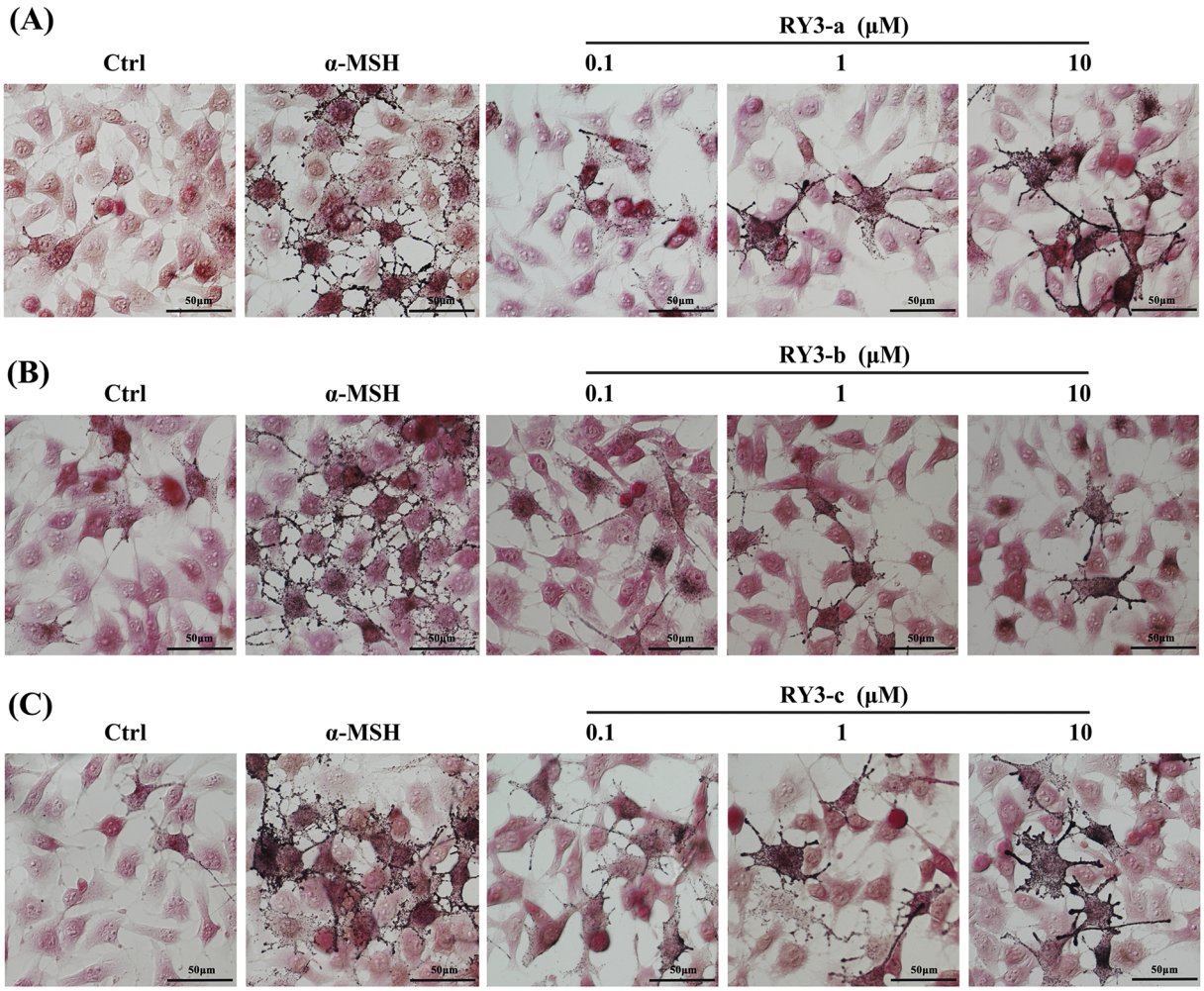

Fig. 4. The melanogenic activities of **RY3-a**, **RY3-b** and **RY3-c** in the B16F10 cell model. B16F10 cells were stained with Masson–Fontana ammoniacal silver stain. B16F10 cells were plated on 13 mm glass coverslips in a six-well plate and then treated with different concentrations of **RY3-a**, **RY3-b** and **RY3-c** for 48 h.

2.3. Investigation of the mechanism of action

2.3.1. Repair of damage induced by oxidative stress

Antioxidant activity in zebrafish and B16F10 cells. Experimental and clinical evidence suggests that oxidative stress plays a vital role in the pathogenesis of the depigmentation process, and high epidermal levels of reactive oxygen species (ROS) have been discovered in vitiligo skin [32]. To investigate whether **RY3-a**, **RY3-b** and **RY3-c** exert melanin synthesis activity through antioxidant activity, the ROS fluorescent probe 2,7-dichlorodihydrofluorescein diacetate (DCFH-DA) and the superoxide-specific fluorescent probe dihydroethidium (DHE) were used in zebrafish and B16F10 cells. As shown in Fig. 7, the difference in green fluorescence between the control group and the H_2O_2 model group was remarkable. Compared with the model group, the ROS content was decreased significantly and concentration-dependently by **RY3-c** treatment at concentrations of 1 μM, 10 μM, 20 μM, and 40 μM, while **RY3-b** treatment exhibited no obvious change in ROS content. This result indicated that **RY3-c** could reverse the ROS content of zebrafish induced by H_2O_2 and could thus exhibit potent antioxidant activity. It was interesting to point out that the fluorescence intensities in the **RY3-a** treatment groups (1 μM, 10 μM, 20 μM, and 40 μM) were clearly lower than that in the H_2O_2-model group, and the ROS content decreased to its lowest level at a concentration of 10 μM while it was increased at concentrations of 20 μM and 40 μM. This result implied

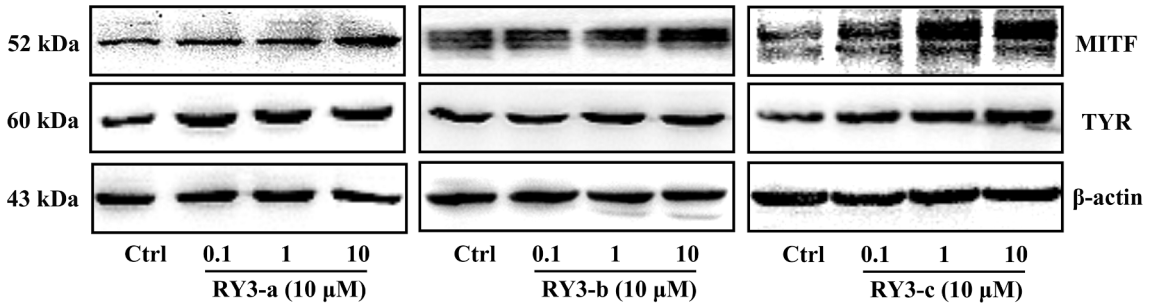

Fig. 5. Effects of **RY3-a**, **RY3-b** and **RY3-c** on the expression levels of TYR and MITF in the B16F10 cell model. The expression levels of TYR and MITF were examined in B16F10 cells by treatment with **RY3-a**, **RY3-b** and **RY3-c** for 48 h. The results were normalized to β-actin expression.

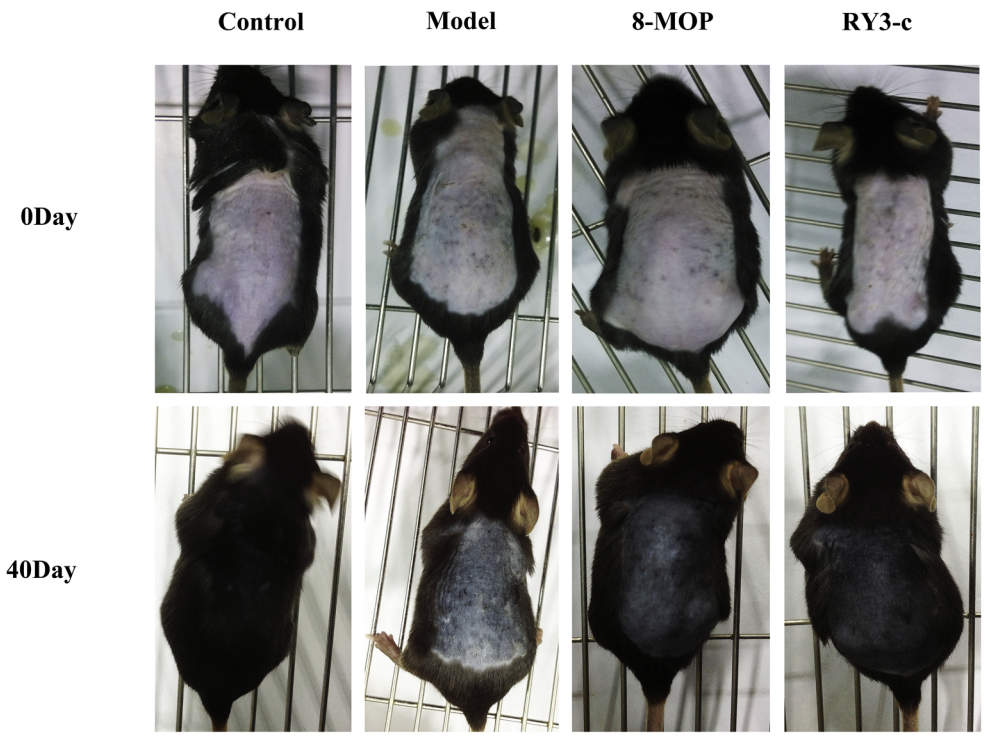

Fig. 6. Effect of compound **RY3-c** on hair growth and hair pigmentation in the vitiligo mouse model induced by hydroquinone. Photographs were taken to document the gross appearance of control and stressed mice on day 0 and day 12, respectively.

that **RY3-a** might induce permanent cell injury or mitochondrial impairment and thus increased ROS production in injured cells at high concentrations of **RY3-a** [33]. This phenomenon indicated that **RY3-a** could exhibit potent antioxidant activity at a low concentration and induce apoptosis and increase ROS production at high concentrations, which is similar to the effects of the flavonoid derivatives galangin, luteolin and myricetin [34]. To illustrate the antioxidant activity of these three compounds, the superoxide-specific fluorescent probe dihydroethidium (DHE) was used in B16F10 cells. Generally, the dimming of red fluorescence indicates good antioxidant activity in comparison with the model and positive control. Images of DHE-stained B16F10 cells are shown in Fig. S1-3 (Supplementary Data (Part 1)). Fig. S1-3 show that the fluorescence intensity of the model group (H_2O_2-treated) was higher than that of the control group, while **RY3-a** and **RY3-c** decreased the superoxide anions detected by lower DHE fluorescence compared to the model group and the vitamin C treatment group. **RY3-b** showed no obvious anti-oxygenation. Obviously, the order of antioxidant activity of these three compounds should be listed as follows: **RY3-c** > **RY3-a** > vitamin C > **RY3-b**.

Inhibition of H_2O_2-induced cytoskeleton damage and apoptosis in B16F10 cells. In vitiligo epidermis, H_2O_2 accumulation has been suggested to be the initial pathogenic event in melanocyte degeneration and early apoptosis [35]. The cytoskeletal damage and apoptosis of H_2O_2-treated B16F10 cells were measured by phalloidin staining and a flow cytometry assay, respectively. As shown in Fig. 8, H_2O_2 treatment markedly induced morphologic changes in B16F10 cells compared with the control group. Fig. 8 also demonstrated that the morphology of B16F10 cells showed no obvious change after H_2O_2 treatment for 4 h, while dendrite tips appeared after treatment with **RY3-a** and **RY3-c** at a concentration of 10 μM. In contrast, cytomorphological alterations of B16F10 cells have been observed by **RY3-b** treatment under the same conditions. As shown in Fig. S1-4 (Supplementary Data (Part 1)), the apoptosis of H_2O_2-treated B16F10 cells was measured by a flow cytometry assay; the flow cytometry assay showed that the apoptotic rate evidently increased from 7.46% to 13.9% after H_2O_2 treatment for 4 h compared to the control group. It is worth noting that pretreatment with **RY3-a** and **RY3-c** could inhibit H_2O_2-induced apoptosis, and the apoptotic rates were reduced to 8.30% and 6.30% compared to the H_2O_2-treatment group (13.9%), respectively, indicating that **RY3-a** and **RY3-c** could repair the cell damage induced by excessive oxidative stress. Clearly, as shown in Fig. 8, **RY3-c** showed better repair ability than **RY3-a**.

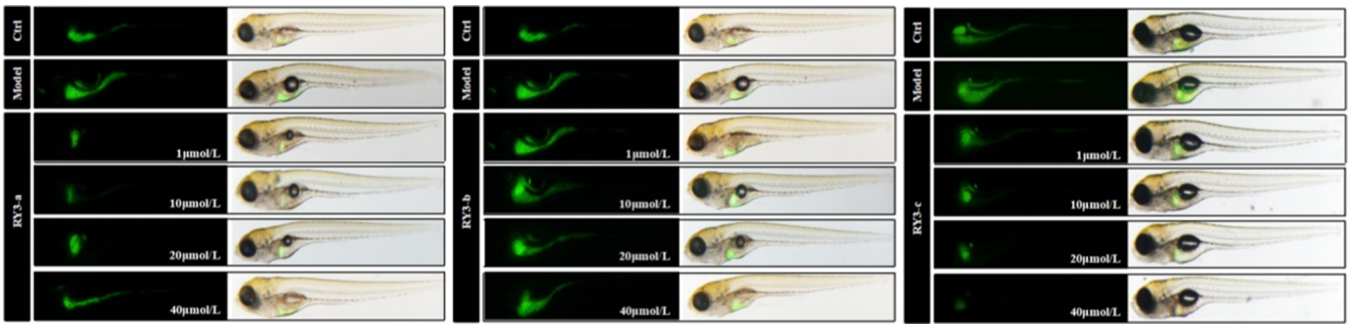

Fig. 7. RY3-a, **RY3-b** and **RY3-c** affected the levels of ROS in the zebrafish model. Zebrafish (7 dpf) were treated with different doses of **RY3-a**, **RY3-b** and **RY3-c** for 24 h and then H_2O_2 (500 μM) for 4 h. DCFH-DA (10 μM) was added to zebrafish for 30 min, and then images were captured.

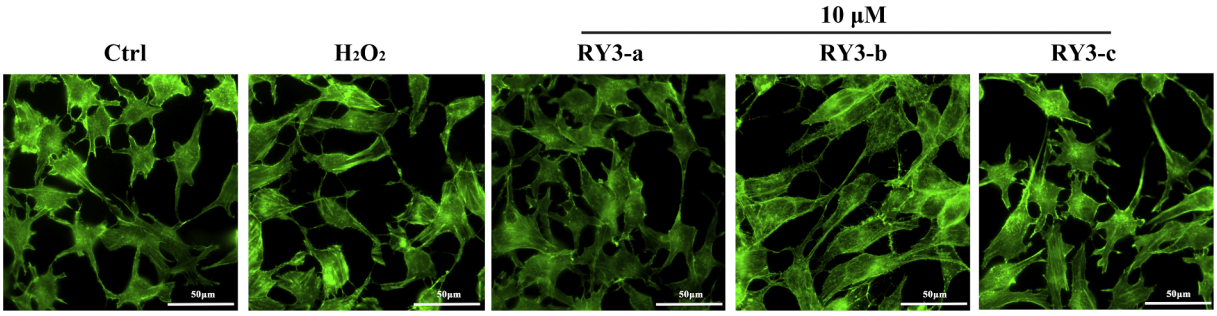

Fig. 8. Effects of **RY3-a**, **RY3-b** and **RY3-c** on H_2O_2-induced cytoskeleton damage of B16F10 cells. B16F10 cells were treated with different doses of **RY3-a**, **RY3-b** and **RY3-c** for 48 h and then H_2O_2 (100 μM) for 4 h. Cells were incubated with 10 μM phalloidin for 30 min. Scale bars, 100 μm.

2.3.2. MAPK signaling pathway of RY3-c

Previous studies have indicated that oxidative stress could mediate the signaling pathways involved in melanin synthesis and vitiligo, including TYR, MITF, and MAPK [10]. To identify the involved signaling pathways, the 3D structure of **RY3-c** was submitted to the versatile web server ChemMapper to study the pharmacology and chemical structure associations [6]. The top 100 related potential targets obtained from ChemMapper were sent to DABID bioinformatics resources, all of the targets interacting with **RY3-c** were mapped onto the KEGG pathways, and cytoscape V3.2.0 software was employed to establish the network (Fig. S3-1 in the Supplementary Data (Part 3)). The network pharmacology research results showed that the MAPK signaling pathway exhibited a high degree of correlation and thus may play an important role in melanin synthesis (Fig. S3-2). Fig. S3-2 shows that c-kit played a key role in melanogenesis via the MAPK signaling pathway and was thus considered to be the target protein for melanin synthesis.

To confirm this signaling pathway, western blot assays were then carried out, and the results are shown in Fig. 9. As shown in Fig. 9A, the expression levels of c-Kit increased in a dose-dependent manner by treatment with **RY3-c** at concentrations of 0.1, 1 and 10 μM. To better understand whether the expression of c-Kit is involved in melanin synthesis, the disruption of c-Kit expression was performed using siRNA. Optimized transfection conditions of B16F10 cells were determined as shown in Fig. 9B. It was found that the combination of 70 μM siRNA and 12.5 μL of Lipo2000 exhibited a better outcome and was thus used for subsequent experiments. As shown in Fig. 9C, the expression of TYR and MITF was reduced significantly by combined siRNA and **RY3-c** treatment, which is consistent with the result obtained by treating the cells with **RY3-c** alone. It is known that c-Kit plays a key role in melanogenesis. To further clarify the mechanism underlying the effect of **RY3-c** on melanogenesis, the MAPK intracellular signal transduction cascade was examined. As shown in Fig. 9D, 10 μM **RY3-c** induced p38 and p-JNK phosphorylation, while the *t*-JNK phosphorylation remained unchanged. p38 phosphorylation increased from 5 min to 120 min, while ERK1/2 phosphorylation was induced at 15 min and reached a peak at 30 min, indicating that **RY3-c** promoted the p38-MAPK and ERK1/2 pathway. To gain further support for this hypothesis, the ERK inhibitor PD98059 and the p38 inhibitor SB203580 were then used. As shown in Fig. 9E and F, western blotting analysis showed that the expression of TYR and MITF was significantly reduced by treatment with the ERK inhibitor PD98059 and the p38 inhibitor SB203580. This result indicated that the p38-MAPK and ERK1/2 pathway is the key regulatory pathway affected by **RY3-c** during melanin synthesis and that c-kit is the key regulatory protein, which is consistent with the above network pharmacological prediction results.

3. Conclusion

In summary, the bioactive component 2′,3,4,4′-tetrahydrochalcone (**CY3-a**) was first isolated from *Vernohia anthelmintica (L.) willd* seeds, and some its analogs **CY3-a-1–CY3-a-15** and **CY3-c** were designed and synthesized as antivitiligo agents. We identified compound **CY3-c**, which exhibited higher melanogenic and antioxidant activities and lower toxicity in comparison with **CY3-a** and butin (**CY3-b**). The vitiligo mouse model study showed that **CY3-c** exhibited better melanogenesis activity compared with the commercial antivitiligo drug 8-MOP. Mechanistic studies showed that **RY3-c** exhibited potent antioxidant activity and could repair cell damage induced by excessive oxidative stress. Further investigation indicated that the p38-MAPK and ERK1/2 pathway is the key pathway affected by **RY3-c** during melanin synthesis and that c-kit is the key regulatory protein, indicating that the MAPK signaling pathway exhibits a high degree of correlation and thus may play an important role in melanin synthesis. This work may provide important information for understanding the antivitiligo mechanism of **RY3-c** and the rational design of antioxidant-based antivitiligo agents.

4. Experimental procedures

4.1. Materials

All of the chemical reagents and solvents used were of analytical grade. The following reagents were purchased from J&K Scientific, Ltd. (Shanghai, China): butin, 2,4-dihydroxyacetophenone, 2-dihydroxyacetophenone, 4-dihydroxyacetophenone, 3,4-dihydroxy-benzaldehyde, 3-dihydroxy-benzaldehyde, and 4-dihydroxy-benzaldehyde. MR spectra were recorded on a Bruker AV-500 NMR spectrometer. Mass spectra were determined on a Q-TOF ESI spectrometer. All compounds were determined by a PE2400 Type II elemental analyzer (U.S. PE firm).

4.2. Chemistry

4.2.1. Isolation procedure for compound RY3-a

RY3-a was isolated from the seeds of *Vernohia anthelmintica (L.) willd*. The seeds were washed with water and then soaked in petroleum ether for 24 h. The seeds were extracted by water, and the crude extract was extracted by diethyl ether and ethyl acetate successively. The ethyl acetate-extracted fraction was separated by octadecylsilyl, and a yellow solid was acquired. Yield, 0.081%; ^{1}HNMR (500 MHz, DMSO-d_6): δ 6.34 (s, 1H, H), 6.46 (d, 1H, J = 20 Hz, H), 6.87 (d, 1H, J = 10 Hz, H), 7.26 (d, 1H, J = 20 Hz, H), 7.33 (s, 1H), 7.72 (d, 2H, J = 10 Hz, H), 8.19 (d, 1H, J = 15 Hz, H), 9.12 (s, 1H), 9.78 (s, 1H), 10.68 (s, 1H), 13.62 (s, 1H). ^{13}CNMR (126 MHz, DMSO-d_6): δ102.45, 107.75, 113.35, 114.45, 115.24, 116.96, 122.20, 127.07, 131.88, 144.69, 145.45, 148.53, 164.94, 166.10, 192.13. Q-TOF (m/z): calculated for $C_{15}H_{12}O_5$ $[M-H]^-$: 271.0760, found: 271.0749.

4.2.2. General synthetic procedure for compounds RY3-a (RY3-a-1-RY3-a-15)

2,4-Dihydroxyacetophenone derivatives (44.7 mmol) in EtOH (20 mL) were added to aqueous potassium hydroxide (41.6 mL, 60% w/

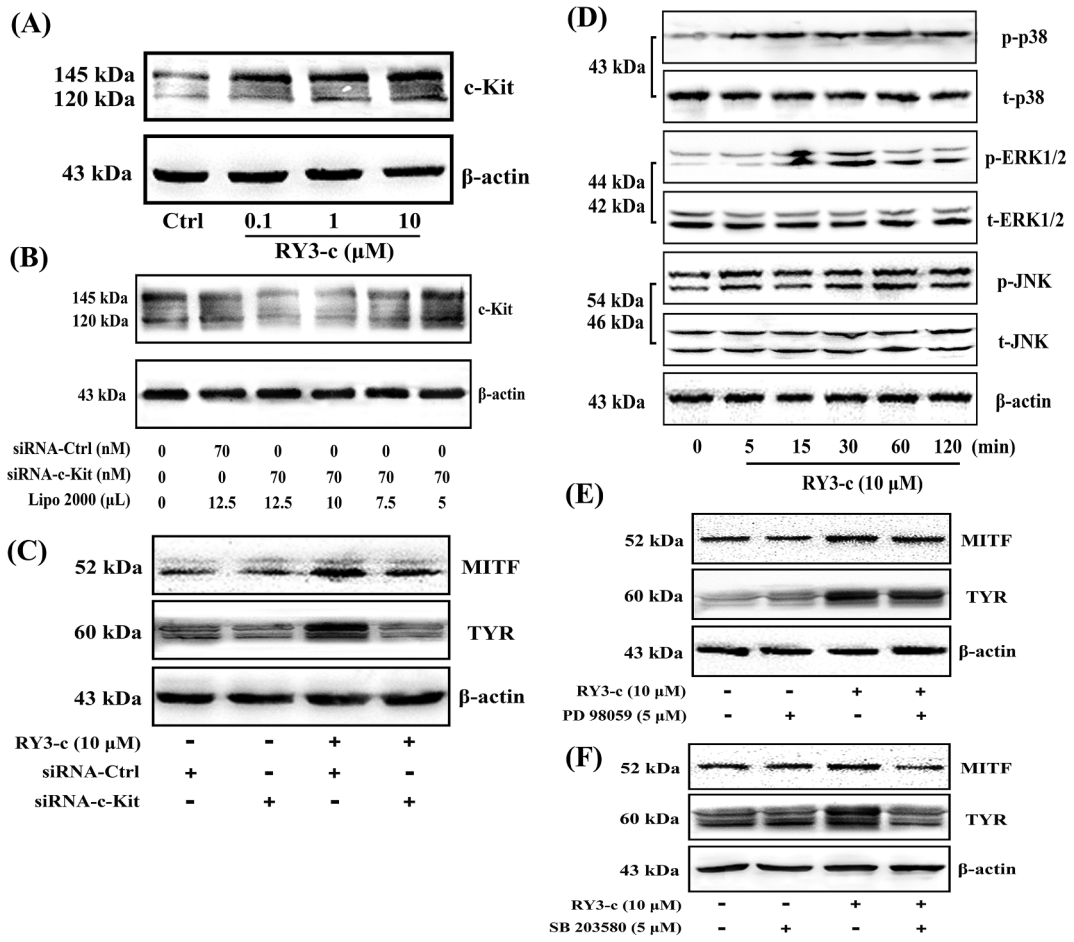

Fig. 9. Effect of compound **RY3-c** on the expression levels of relevant proteins in B16F10 cells. (A) Effect of compound **RY3-c** on the expression of c-kit. (B) Inhibition of c-kit expression using siRNA transfected into B16F10 cells. (C) Effect of compound **RY3-c** on the expression of MITF and TYR after c-kit siRNA treatment in B16F10 cells. (D) Effect of compound **RY3-c** on the expression of p38, ERK, and JNK and the phosphorylation of p38, ERK, and JNK. (E) Effect of compound **RY3-c** on the expression of MITF and TYR after PD98059 treatment in B16F10 cells. (F) Effect of compound **RY3-c** on the expression of MITF and TYR after SD203580 treatment in B16F10 cells.

w) under magnetic stirring for 10 min at room temperature followed by the addition of 2,3-dihydroxybenzaldehyde derivatives (45.9 mmol). The mixture was stirred magnetically at 85 °C for 2 h and then poured onto ice. The reaction mixture was acidified to a pH = 4 using cold hydrochloric acid and extracted with EtOAc. The combined EtOAc extracts were washed with brine solution, dried with Na_2SO_4 and concentrated under reduced pressure. Purification of the crude product by flash chromatography (20% EtOAc/hexane) yielded **RY3-a-1–RY3-a-15**.

RY3-a-1: Yield, 73.2%; ^{1}HNMR (500 MHz, DMSO-d_6): δ 6.30 (m, 1H, J = 10 Hz), 6.43 (dd, 1H, J = 10 Hz), 6.85 (d, 2H, J = 10 Hz), 7.75 (d, 4H, J = 10 Hz), 8.16 (dd, 1H, J = 10 Hz), 10.14 (s, 1H), 10.68 (s, 1H), 13.62 (s, 1H). ^{13}CNMR (126 MHz, DMSO-d_6): δ 103.10, 108.58, 113.51, 116.33, 117.90, 126.24, 133.28, 131.66, 160.74, 165.42, 166.28, 192.01; Q-TOF (m/z): calculated m/z for $C_{15}H_{12}O_6$ [M-H]$^-$: 255.0770, found: 255.0674.

RY3-a-2: Yield, 65.2%; ^{1}HNMR (500 MHz, DMSO-d_6): δ 6.30 (d, 1H, J = 5 Hz), 6.42 (m, 1H, J = 15 Hz), 6.88 (m, 1H, J = 10 Hz), 7.26 (m, 2H, J = 20 Hz), 7.32 (d, 1H, J = 10 Hz), 7.70 (d, 1H, J = 20 Hz), 7.88 (d, 1H, J = 25 Hz), 8.18 (d, 1H, J = 15 Hz), 9.63 (s, 1H), 10.75 (s, 1H), 13.38 (s, 1H).; ^{13}CNMR (126 MHz, DMSO-d_6): δ103.08, 108.77, 113.54, 115.92, 118.35, 120.44, 121.63, 130.35, 133.63, 136.39, 144.38, 158.21, 165.42, 166.25, 191.95; Q-TOF (m/z): calculated m/z for $C_{15}H_{12}O_6$ [M-H]$^-$: 255.0770, found: 255.0675.

RY3-a-3: Yield, 80.1%;^{1}HNMR (500 MHz, DMSO-d_6): δ 6.34 (d, 1H, J = 5 Hz), 6.46 (dd, 1H, J = 10 Hz), 7.49 (dd, 3H, J = 5 Hz), 7.82 (d, 1H, J = 15 Hz), 7.92 (dd, 2H, J = 10 Hz), 8.00 (d, 1H, J = 15 Hz), 8.22 (d, 1H, J = 10 Hz), 10.74 (s, 1H), 13.41 (s, 1H);^{13}CNMR (126 MHz, DMSO-d_6): δ 103.12, 108.84, 113.50, 121.83, 129.41, 129.48, 131.15, 133.65, 135.13, 144.10, 165.91, 166.32, 191.94; Q-TOF (m/z): calculated m/z for $C_{15}H_{12}O_3$ [M-H]$^-$: 239.0780, found: 239.0718.

RY3-a-4: Yield, 77.6%; ^{1}HNMR (500 MHz, DMSO-d_6): δ 6.81 (m, 1H, J = 15 Hz), 6.90 (s, 2H), 7.23 (m, 1H, J = 5 Hz), 7.57 (m, 2H, J = 50 Hz), 8.02 (d, 2H, J = 10 Hz), 9.03 (s, 1H), 9.64 (s, 1H), 10.34 (s, 1H); ^{13}CNMR (126 MHz, DMSO-d_6): δ115.77, 115.88, 116.22, 118.94, 122.28, 126.96, 129.98, 131.34, 144.08, 146.04, 148.86, 162.32, 187.52; Q-TOF (m/z): calculated m/z for $C_{15}H_{12}O_4$ [M-H]$^-$: 255.0770, found: 255.0687.

RY3-a-5: Yield, 81.2%;^{1}HNMR (500 MHz, DMSO-d_6): δ 6.84 (d, 1H, J = 10 Hz), 6.99 (m, 2H, J = 15 Hz), 7.24 (d, 1H, J = 10 Hz), 7.32 (s, 1H), 7.55 (t, 1H, J = 20 Hz), 7.74 (s, 1H), 8.23 (d, 1H, J = 20 Hz); ^{13}CNMR (126 MHz, DMSO-d_6): δ 116.28, 117.95, 118.17, 119.51, 121.15, 123.39, 126.40, 131.04, 136.43, 146.35, 146.63, 162.47, 193.85; Q-TOF (m/z): calculated m/z for $C_{15}H_{12}O_4$ [M-H]$^-$: 255.0770, found: 255.0603.

RY3-a-6: Yield, 53.2%; ^{1}HNMR (500 MHz, DMSO-d_6): δ 6.84 (d, 1H, J = 5 Hz), 7.19 (dd, 1H, J = 5 Hz), 7.28 (s, 1H,), 7.32 (s, 1H), 7.57 (t, 1H, J = 15 Hz), 7.61 (s, 1H), 7.66 (t, 1H, J = 15 Hz), 8.11 (m, 2H, J = 10 Hz);^{13}CNMR (126 MHz, DMSO-d_6):δ 115.97, 116.32, 118.76, 122.76, 126.54, 128.76, 129.19, 133.20, 138.57, 145.53, 146.21, 149.59; Q-TOF (m/z):calculated m/z for $C_{15}H_{12}O_3$ [M-H]$^-$: 239.0780, found: 239.1026.

RY3-a-7: Yield, 84.2%; ^{1}HNMR (500 MHz, DMSO-d_6): δ 6.87 (m, 4H, J = 40 Hz), 7.68 (dd, 4H, J = 50 Hz), 8.04 (dd, 2H, J = 15 Hz), 10.20 (s, 1H); ^{13}CNMR (126 MHz, DMSO-d_6): δ 115.78, 116.27, 119.04, 126.47, 129.95, 131.18, 131.40, 143.65, 160.30, 162.38, 187.57. Q-TOF (m/z): calculated m/z for $C_{15}H_{12}O_3$ [M-H]$^-$: 239.0780, found: 239.0817.

RY3-a-8: Yield, 77.6%;^{1}HNMR (500 MHz, DMSO-d_6): δ 6.86 (d, 2H, J = 10 Hz), 7.00 (t, 2H, J = 5 Hz), 7.55 (m, 1H, J = 25 Hz), 7.78 (m, 2H, J = 25 Hz), 7.83 (d, 2H, J = 15 Hz), 8.25 (d, 1H, J = 5 Hz), 10.22 (s, 1H,), 12.79 (s, 1H); ^{13}CNMR (126 MHz, DMSO-d_6): δ116.40, 118.20, 119.53, 121.05, 126.06, 131.12, 131.99, 136.57, 146.13, 161.11, 162.54, 194.04; Q-TOF (m/z): calculated m/z for C_{15} $H_{12}O_3$ [M-H]$^-$: 239.0780, found: 239.0942.

RY3-a-9: Yield, 71.3%;^{1}HNMR (500 MHz, DMSO-d_6): δ 6.86 (d, 2H, J = 10 Hz), 7.57 (t, 2H, J = 20 Hz), 7.66 (t, 1H, J = 10 Hz), 7.74 (m, 4H, J = 15 Hz), 8.12 (d, 2H, J = 5 Hz), 10.12 (s, 1H,); ^{13}CNMR (500 MHz, DMSO-d_6): δ116.32, 119.01, 126.26, 128.80, 129.18, 131.49, 133.26, 138.47, 145.00, 160.65; Q-TOF (m/z): calculated m/z for $C_{15}H_{12}O_2$ [M-H]$^-$: 223.0890, found: 223.0990.

RY3-a-10: Yield, 64.2%;^{1}HNMR (500 MHz, DMSO-d_6): δ 6.88 (ddd, 1H, J = 20 Hz), 6.92 (m, 2H, J = 5 Hz), 7.21 (m, 1H, J = 5 Hz), 7.28 (m, 2H, J = 20 Hz), 7.60 (d, 1H, J = 15 Hz), 7.81 (d, 1H, J = 15 Hz), 8.07 (m, 2H, J = 30 Hz), 9.60 (s, 1H), 10.41 (s, 1H); ^{13}CNMR (500 MHz, DMSO-d_6): δ 115.60, 115.87, 117.98, 120.13, 122.45, 129.62, 130.33, 131.63, 136.66, 143.43, 158.20, 162.65, 187.65; Q-TOF (m/z): calculated m/z for $C_{15}H_{12}O_3$[M-H]$^-$: 239.0780, found: 239.0740.

RY3-a-11: Yield, 60.3%;^{1}HNMR (500 MHz, DMSO-d_6): δ 6.86 (d, 2H, J = 10 Hz), 6.91 (d, 2H, J = 10 Hz), 7.65 (s, 1H,), 7.69 (s, 1H), 7.72 (d, 2H, J = 5 Hz), 8.05 (d, 2H, J = 5 Hz), 10.01(s, 1H), 10.32 (s, 1H); ^{13}CNMR (126 MHz, DMSO-d_6):115.79, 116.27, 119.04, 126.48, 129.96, 131.29, 143.65, 160.30, 162.38, 187.58; Q-TOF (m/z): calculated m/z for $C_{15}H_{12}O_3$ [M-H]$^-$: 239.0780, found: 239.0907.

RY3-a-12: Yield, 52.3%; ^{1}HNMR (500 MHz, DMSO-d_6) δ 6.90 (m, 1H, J = 10 Hz), 7.26 (m, 2H, J = 30 Hz), 7.33 (d, 1H, J = 10 Hz), 7.59 (t, 2H, J = 15 Hz), 7.68 (m, 2H, J = 25 Hz), 7.84 (d, 1H, J = 15 Hz), 8.15 (m, 2H, J = 5 Hz), 9.64(s, 1H). ^{13}CNMR (126 MHz, DMSO-d_6) δ 115.76, 118.33, 120.36, 122.44, 128.98, 129.28, 130.38, 133.59, 136.42, 138.10, 144.76, 158.23, 189.76; Q-TOF (m/z):calculated m/z for $C_{15}H_{12}O_2$[M-H]$^-$: 223.0890, found: 223.0866.

RY3-a-13: Yield, 55.6%;^{1}HNMR (500 MHz, DMSO-d_6): δ 6.93 (d, 2H, J = 10 Hz), 7.46 (m, 3H, J = 20 Hz), 7.70 (d, 1H, J = 15 Hz), 7.88 (dd, 2H, J = 10 Hz), 7.92 (dd, 1H, J = 15 Hz), 8.11 (s,2H), 10.43(s, 1H);^{13}CNMR (126 MHz, DMSO-d_6); ^{13}CNMR (126 MHz, DMSO-d_6): δ 115.89, 122.66, 129.16, 129.37, 129.62, 130.78, 131.67, 135.39, 143.18, 162.70, 187.66. Q-TOF (m/z): calculated m/z for $C_{15}H_{12}O_2$[M-H]$^-$: 223.0890, found: 223.0802.

RY3-a-14: Yield, 63.6%; ^{1}HNMR (500 MHz, DMSO-d_6): δ 7.03 (dt, 2H, J = 20 Hz), 7.49 (m, 3H, J = 10 Hz), 7.59 (t, 1H, J = 10 Hz), 7.86 (d, 2H, J = 15 Hz), 8.06 (d, 1H, J = 20 Hz),8.27 (dd,1H, J = 20 Hz),12.53 (s,1H); ^{13}CNMR (126 MHz, DMSO-d_6): δ 118.21, 119.65, 122.29, 129.53, 131.36, 134.93, 136.79, 145.25, 162.36, 194.11; Q-TOF (m/z): calculated m/z for $C_{15}H_{12}O_2$ [M-H]$^-$:223.0890, found: 223.0850.

RY3-a-15: Yield, 70.3%; ^{1}HNMR(500 MHz, DMSO-d_6):δ 7.49 (m, 3H, J = 5 Hz), 7.60 (t, 2H, J = 15 Hz), 7.70 (t, 1H, J = 15 Hz), 7.78 (t, 1H, J = 15 Hz), 7.92 (m, 2H, J = 5 Hz), 7.96 (d, 1H, J = 20 Hz), 8.17 (m,2H, J = 10 Hz);^{13}CNMR (126 MHz, DMSO-d_6): δ 122.62, 129.01, 129.29, 129.38, 129.41, 131.13, 133.63, 144.52, 189.74; Q-TOF (m/z): calculated m/z for $C_{15}H_{12}O$ [M+Na]$^+$: 231.0830, found: 231.0815.

4.2.3. Synthesis of RY3-c

2,4-Dihydroxyacetophenone was dissolved in dry THF, and the mixture was cooled to −60 °C under an atmosphere of dry nitrogen. LiHMDS (1.6 M in hexane, 30 mmol) was added dropwise, and the reaction was stirred for 45 min at −30 °C. The phenolic hydroxyl groups of 3,4-dihydroxybenzoic acid ethyl ester (1.82 g, 10 mmol) were protected by benzyl (**RY3-c**) and dissolved in dry THF (20 mL). The mixture was then cooled to −60 °C and to 4.36 g of **RY3-c**, and dry THF (40 mL) was added dropwise. This mixture was stirred for another 45 min at −60 °C and then incubated at room temperature overnight. The reaction mixture was poured on ice and acidified with 2.0 M HCl. The THF was removed, the crude 1-(3,4-bis-benzyloxy-phenyl)-3-(2,4-dihydroxy-phenyl)-propane-1,3-dione was dissolved in 2-propanol (50 mL), 0.5 g Dowex W50 × 8 (H^+ form) was added, and the reaction was heated under reflux for 24 h under an atmosphere of dry nitrogen. The solids were filtered, and then the reaction mixture was poured on water. The solids were filtered and dissolved in MeOH (50 mL), and Pd-C (1 g) was added under an atmosphere of dry hydrogen at room temperature overnight. The solids were filtered and MeOH was removed. Purification of the crude product by flash chromatography (30% EtOAc/hexane) yielded **RY3-c** (1.28 g, 32.4%) as a white solid. **RY3-c**: ^{1}HNMR (500 MHz, DMSO-d_6): δ 6.62 (s, 1H), 6.92 (m, 2H, J = 10 Hz), 6.95 (d, 1H, J = 5 Hz), 7.40 (dd, 2H, J = 10 Hz), 7.88 (d, 1H, J = 10 Hz), 9.61 (s, 2H), 10.77 (s, 1H). ^{13}CNMR (126 MHz, DMSO-d_6): δ102.83, 104.97, 113.66, 115.24, 116.47, 118.99, 122.62, 126.94, 146.16, 149.61, 157.81, 163.02, 163.07, 176.63. Q-TOF (m/z): calculated m/z for $C_{15}H_{10}O_5$ [M-H]$^-$: 269.0500, found: 269.0536.

4.3. Biological assays

The procedures for the biological assays are described in the Supplementary Data (Part 1–Part 3). The materials, instrumentation and methods for the cytotoxicity assay, apoptosis analysis and western blot assays were reported previously [36–38]. Animal handling procedures conformed to the guidelines of the animal ethics committee of the Chinese Ministry of Health and the animal experiment standards, and they were approved by the animal management committee of China Pharmaceutical University.

Disclosure of potential conflicts of interest

The authors declare no competing financial interests.

Acknowledgments

This study was supported by the National Natural Science Foundation of China (No. 81874331), the Postgraduate Research & Practice Innovation Program of Jiangsu Province (KYCX17_0669) and the Open Project for Chemistry and Molecular Engineering of Medicinal Resources (Guangxi Normal University) (CMEMR2017-B02).

Appendix A. Supplementary material

Supplementary data to this article can be found online at https://doi.org/10.1016/j.bioorg.2019.03.054.

References

[1] E. Nicolaidou, A.D. Katsambas, Pigmentation disorders: hyperpigmentation and hypo-pigmentation, Clin. Dermatol. 32 (2014) 66–72.
[2] N. Malhotra, M. Dytoc, The pathogenesis of vitiligo, J. Cutan. Med. Surg. 17 (2013) 153–172.
[3] I.C.L. Poole, P.K. Das, R.M.J.G.J. van den Wijngaard, J.D. Bos, W. Westerhof, Review of the etiopathomechanism of vitiligo: a convergence theory, Exp. Dermatol. 2 (1993), 145–153.
[4] K.U. Schallreuter, Successful treatment of oxidative stress in vitiligo, Skin Pharmacol. Phys. 12 (1999) 132–138.
[5] V. Maresca, M. Roccella, F. Roccella, E. Camera, G. Del Porto, S. Passi, P. Grammatico, M. Picardo, Increased sensitivity to peroxidative agents as a possible pathogenic factor of melanocyte damage in vitiligo, J. Invest. Dermatol. 109 (1997) 310–313.
[6] N.C. Laddha, M. Dwivedi, M.S. Mansuri, A.R. Gani, M. Ansarullah, A.V. Ramachandran, S. Dalai, R. Bequm, Vitiligo: interplay between oxidative stress and immune system, Exp. Dermatol. 22 (2013) 245–250.

[7] A.A. Shah, A.A. Sinha, Oxidative stress and autoimmune skin disease, Eur. J. Dermatol. 23 (2013) 5–13.
[8] L. Guerra, E. Dellambra, S. Brescia, D. Raskovic, Vitiligo: pathogenetic hypotheses and targets for current therapies, Curr. Drug. Metab. 11 (2010) 451–467.
[9] S.J. Glassman, S.B. Heidelberg, ROS and Vitiligo, 2014, 3677.
[10] A. Slominski, D.J. Tobin, S. Shibahara, J. Wortsman, Melanin pigmentation in mammalian skin and its hormonal regulation, Physiolo. Rev. 84 (2004) 1155–1228.
[11] G. Akoglu, S. Emre, A. Metin, A. Akbas, A. Yorulmaz, S. Isikouqlu, S. Sener, F. Kilinc, Evaluation of total oxidant and antioxidant status in localized and generalized vitiligo, Clin. Exp. Dermatol. 38 (2013) 701–706.
[12] O. Szczurko, N. Shear, A. Taddio, H. Boon, Ginkgo biloba for the treatment of vitilgo vulgaris: an open label pilot clinical trial, BMC. Complem. Altern. M. 11 (2011) 21–29.
[13] Y.S. Tuerxun Drug Standard of Ministry of Public Health of the People's Republic of China (Uygur Medicine), Urumqi Science and Technology Publishing House: Xinjiang. 1999, 150–153.
[14] D.R. Shi, L.S. Ha, X. Ru, H.F. Gan, J.L. Liu, X.M. Pu, Clinical efficacy of treatment of Vernonia anthelmintica (L.) Willd on vitiligo, Xinjiang Med. J. 33 (2003) 51–52.
[15] Z.Q. Ma, H. Hu, T.T. He, H. Guo, M.Y. Zhang, M.W. Chen, Y.T. Wang, An assessment of traditional Uighur medicine in current Xinjiang region (China), Afr. J. Tradit. Complem. 11 (2014) 301–314.
[16] A.K. Patel, S.A. Bhalerao. Ethnobotany, phytochemistry and pharmacological evaluation of vernonia anthelmintica (l.) willd.: an overview, Asian J. Sci. Technol. 8(2017) 6258–6262.
[17] S.X. Huo, Q. Wang, X.M. Liu, C.H. Ge, L. Gao, X.M. Peng, M. Yan, The effect of butin on the vitiligo mouse model induced by hydroquinone, Phytother. Res. 31 (2017) 740–746.
[18] H. Emily, W. Jonathan, D. Thuy, K. Reid, S. Lindsey, H. Quintin, H. Grace, C. Austin, M. Lili, P. Stefan, Hydroxylated chalcones with dual properties: Xanthine oxidase inhibitors and radical scavengers, Bioorgan. Med. Chem. 24 (2016) 578–587.
[19] M. Deodhar, D.S. Black, N. Kumar, Acid-catalyzed stereoselective rearrangement and dimerization of flavenes: synthesis of dependensin, J. Cheminf. 63 (2007) 5227–5235.
[20] J.P. Lv, X.M. Zha, S.L. Pang, H.P. Jia, Y. Zhang, J. Shang, Synthesis and melanogenesis evaluation of 3',4',7-trihydroxyflavanone derivatives and characterization of flavanone-BODIPY, Bioorgan. Med. Chem. Lett. 25(2015), 1607–1610.
[21] J. Med. Chem. 55 (10) (2012) 4551–4567, https://doi.org/10.1021/jm201107g.
[22] T.Y. Choi, J.H. Kim, D.H. Ko, C.H. Kim, J.S. Hwang, S. Ahn, S.Y. Kim, C.D. Kim, J.H. Lee, T.J. Yoon, Zebrafish as a new model for phenotype-based screening of melanogenic regulatory compounds, Pigm. Cell. Res. 20 (2010) 120–127.
[23] E. Camp, M. Lardelli, Tyrosinase gene expression in zebrafish embryos, Dev. Genes. Evol. 211 (2001) 150–153.
[24] J. Oh, J. Kim, J.H. Jang, S. Lee, C.M. Park, W.K. Kim, J.S. Kin, Novel (1E,3E,5E)-1,6-bis (Substituted phenyl) hexa-1,3,5-triene Analogs Inhibit Melanogenesis in B16F10 Cells and Zebrafish, Int. J. Mol. Sci. 19 (2018) 1067–1078.
[25] J.H. Ha, Y.J. Jeong, S.H. Xuan, J.Y. Lee, J. Park, S.N. Park, Methyl-2-acetylamino-3-(4-hydroxyl-3,5-dimethoxybenzoylthio) propanoate suppresses melanogenesis through ERK signaling pathway mediated MITF proteasomal degradation, J. Dermatol. Sci. 91 (2018) 142–152.
[26] R. Zhang, R. Fan, Z. Cheng, X. Tian, J. Liu, Regulation of TYR and MITF mRNA expression by CDK5 in alpaca melanocytes, Chinese J. Anim. Veter. Sci. 42 (2011) 1712–1717.
[27] Y. Wakabayashi, H. Nakajima, G. Imokawa, Abrogating effect of N-linked carbohydrate modifiers on the stem cell factor and endothelin-1-stimulated epidermal pigmentation in human epidermal equivalents, J. Dermatol. Sci. 69 (2013) 215–228.
[28] F. Zhang, W. Qin, J.P. Zhang, C.Q. Hu, Antibiotic toxicity and absorption in zebrafish using liquid chromatography-tandem mass spectrometry, Plos One 10 (2015) e0124805.
[29] N.A. Ducharme, D.M. Reif, J.A. Gustafsson, M. Bondesson, Reprod Toxicol, Comparison of toxicity values across zebrafish early life stages and mammalian studies: implications for chemical testing, Reprod. Toxicol. 55 (2015) 3–10.
[30] W.H. Peng, Y.C. Lee, Y.P. Chau, K.S. Lu, H.N. Kung, Short-term exposure of zebrafish embryos to arecoline leads to retarded growth, motor impairment, and somite muscle fiber changes, Zebrafish 12 (2015) 58–70.
[31] S.X. Huo, X.M. Liu, C.H. Ge, L. Gao, X.M. Peng, P.P. Zhao, M. Yan, The effects of galangin on a mouse model of vitiligo induced by hydroquinone, Phytother. Res. 28 (2015) 1533–1538.
[32] R. Colucci, F. Dragoni, S. Moretti, Oxidative stress and immune system in vitiligo and thyroid diseases, Oxid. Med. Cell. Longev. (2015) 631927.
[33] M.L. Dell'Anna, V. Maresca, S. Briganti, E. Camera, M. Falchi, M. Picardo, Mitochondrial impairment in peripheral blood mononuclear cells during the active phase of vitiligo, J. Invest. Dermatol. 117 (2001) 908–913.
[34] N.L. Vukovic, A.D. Obradovic, M.D. Vukic, D. Jovanovic, P.M. Djurjevic, Cytotoxic, proapoptotic and antioxidative potential of flavonoids isolated from propolis against colon (HCT-116) and breast (MDA-MB-231) cancer cell lines, Food. Res. Int. 106 (2018) 71–80.
[35] J. Gong, C. Cai, X. Liu, H. Jiang, D. Gao, H. Li, ChemMapper: a versatile web server for exploring pharmacology and chemical structure association based on molecular 3D similarity method, Bioinformatics 29 (2013) 1827–1829.
[36] F.F. Ping, J. Shang, J. Zhou, J. Song, L. Zhang, Activation of neurokinin-1 receptor by substance P inhibits melanogenesis in B16–F10 melanoma cells, Int. J. Biochem. Cell. B. 44 (2012) 2342–2348.
[37] J. Zhou, J.Y. Feng, W. Qian, J. Shang, Calcitonin gene-related peptide cooperates with substance P to inhibit melanogenesis and induces apoptosis of B16F10 cells, Cytokines 74 (2015) 137–144.
[38] S. Liao, J. Lv, J. Zhou, P.K. Kalavagunta, J. Shang, Effects of two chronic stresses on mental state and hair follicle melanogenesis in mice, Exp. Dermatol. 26 (2017) 1083–1090.